

## Electron Tunneling and Band Structure of $\text{SrTiO}_3$ and $\text{KTaO}_3$ <sup>†</sup>

Z. Sroubek\*

*Department of Physics, University of California, Los Angeles, California 90024*

(Received 24 February 1970)

The tunneling characteristics of In-SrTiO<sub>3</sub>:Nb and In-KTaO<sub>3</sub>:Ca Schottky barriers have been studied at different temperatures and for different concentrations of carriers. The plot of differential resistivity shows a distinct peak at forward biases which is attributed to the critical point in the density of states at the bottom of the semiconductor conduction band. From the position of the peak, the density-of-states effective masses  $m_d$  have been found to be  $1.3m_0$  in SrTiO<sub>3</sub> and  $0.69m_0$  in KTaO<sub>3</sub>. In combination with magnetoresistance data, the widths of the conduction bands have been determined. The over-all widths of the  $d$  bands are about 3.4 and 6.8 eV for SrTiO<sub>3</sub> and KTaO<sub>3</sub>, respectively. Finally, in the theoretical part, the conduction-band structure of transition-metal perovskites is discussed.

### I. INTRODUCTION

The transition-metal oxides exhibit a wide variety of electrical and magnetic properties which are interesting from practical and theoretical points of view. For example, one of the most striking properties of some of these materials, namely, vanadium and titanium oxides, is a sudden transition from high-temperature metallic behavior to low-temperature semiconducting behavior with a discontinuous change in conductivity of several orders of magnitude. The problem of the transition has been of considerable interest for several years but there has been insufficient experimental data in the past to allow unambiguous conclusions to be reached, not only on the nature of the transition, but even on the basic electronic properties of transition-metal oxides. Difficulties in growing pure stoichiometric single crystals are the main obstacle in experimental study of both vanadium and titanium oxides and are the reasons why the experimental data and their interpretation have often been contradictory. Moreover, the low symmetry and high carrier concentration lead to very complex Fermi surfaces (often several bands are overlapping), details of which are presently extremely difficult to determine experimentally.

For this reason, it is worthwhile to investigate the electronic structure of closely related, but substantially simpler systems, which retain the basic electronic properties of a transition-metal oxide but are technically easier to study.

Crystals of SrTiO<sub>3</sub>, KTaO<sub>3</sub>, and TiO<sub>2</sub> are suitable for this purpose. Compared to the conducting oxides mentioned above, they are excellent insulators in stoichiometric state and do not contain any valence  $d$  electrons. (Ti<sup>4+</sup> and Ta<sup>5+</sup> have closed shells.) All three crystals can be easily doped with donorlike impurities which provide controllable amounts of carriers in previously unoccupied "band"  $3d$  states

of Ti<sup>3+</sup> and  $5d$  states of Ta<sup>4+</sup>. Relatively small carrier concentrations exclude any complication due to correlation effects which may exist in concentrated materials and the experiments on the electronic structure can be interpreted in terms of pure metal ion-oxygen-metal ion and metal ion-metal ion transfers. The understanding of these two transfer processes is essential to the understanding of the electronic structure of transition-metal oxides.

The SrTiO<sub>3</sub> and KTaO<sub>3</sub> crystals when conveniently doped are in many respects prototypes of transition-metal oxide semiconductors. They possess a simple cubic perovskite structure in which the direct cation-cation interaction can be neglected and the bandwidth is entirely due to cation-anion-cation interactions. Both exhibit metallic conductivity down to 1 °K without any indication of a carrier freezeout. The TiO<sub>2</sub> crystal, which resembles more closely some transition-metal oxides of current interest (e.g., VO<sub>2</sub>), has more complicated structure with both cation-cation and cation-anion-cation interactions contributing to the bandwidth. For reasons not yet understood, it is impossible to dope TiO<sub>2</sub> crystals with shallow donors, and the crystals are nonconducting at low temperatures.

In the present paper the band structures of SrTiO<sub>3</sub> and KTaO<sub>3</sub> have been studied using tunneling techniques. Tunneling experiments provide a direct measurement of the density-of-states effective mass, in principle, at any temperature, and even in very heavily doped materials. These are obvious advantages in comparison with the technique of cyclotron resonance which is applicable only for materials with extremely small carrier concentration and with long carrier lifetime. The last requirement is the most difficult to fulfill in oxides, and cyclotron resonance has, in fact, been observed only in KTaO<sub>3</sub>.<sup>1</sup> The knowledge of the density-of-states effective mass is, however, not sufficient for a complete determination of the effective-mass

tensor and tunneling data must be combined with results of other experiments (magnetoresistance effect, Shubnikov-de Haas oscillations) in order to obtain a complete picture of the band properties. The applicability of the tunneling technique for determination of effective masses in perovskite semiconductors will be checked in the paper by comparing our tunneling data and recent magnetoresistance measurement<sup>2</sup> on  $\text{KTaO}_3$  with cyclotron resonance data.<sup>1</sup>

We shall discuss in more detail the case of relatively narrow-band strontium titanate. Preliminary results of the  $\text{SrTiO}_3$  tunneling experiments (concentration dependence of the Fermi energy  $\mu_F$ ) have already been described in a previous publication.<sup>3</sup> We have extended these measurements to different temperatures and to junctions formed with different counterelectrode metals. On the theoretical side, we will suggest conduction-band structure for  $\text{SrTiO}_3$  which is consistent with the experimental results and which is at variance with some conclusions of previous transition-metal oxide band calculations.<sup>4</sup>

## II. EXPERIMENTAL

The tunneling experiments on  $\text{SrTiO}_3$  have been done on Nb-doped single crystals cut from two boules with two different  $\text{Nb}_2\text{O}_5$  doping. The boules were grown and supplied by the National Lead Co. The carrier concentration was determined from Hall measurements to be  $7 \times 10^{18}/\text{cm}^3$  in one boule and  $5 \times 10^{19}/\text{cm}^3$  in the other. The crystals of  $\text{KTaO}_3$  have been grown in our laboratory. A charge of pure  $\text{K}_2\text{CO}_3$  and  $\text{Ta}_2\text{O}_5$  mixed in mole ratio 1.7 was melted on air in a platinum crucible at  $1400^\circ\text{C}$  and the temperature was afterwards slowly lowered at  $5^\circ\text{C}$  per hour. In contrast to previous reports,<sup>5,6</sup> the crystals grown from undoped charge were transparent and perfectly insulating. The free carriers were introduced by adding a small amount of  $\text{CaCO}_3$  into the starting charge. The  $\text{Ca}^{2+}$  ions substitute the  $\text{K}^+$  ions and act as a very shallow donor – no carrier freezeout has been observed, even at the lowest of temperatures ( $1^\circ\text{K}$ ).

The  $\text{SrTiO}_3$  and  $\text{KTaO}_3$  samples were cut from single-crystal material in the form of a bar typically  $0.8 \times 0.8 \times 15$  mm in dimensions. The crystals were oriented such that a (100) cleavage surface was produced by breaking the bar in the middle. Two Ohmic contacts were made on each side of the bar using indium solder and ultrasonic soldering iron. Tunneling contacts were made by cleaving the sample in a vacuum of  $2 \times 10^{-6}$  Torr and by evaporating suitable metal (Pb, Sn, and Bi) or by cleaving in air and by pressing immediately freshly cut indium metal against the cleavage plane. The last method is simple and highly successful and

was used in the majority of experiments. The evaporated contacts were mainly used to check the reproducibility of tunneling structures and their independence on the barrier height.

The occurrence of tunneling was inferred from the observation of the BCS energy gap in the counterelectrode metal. The gap was seen in all junctions.

The slope  $dV/dI$  of the voltage-current characteristic of the junctions has been measured using conventional techniques. A steady current and a small ac were driven through the junction by a high impedance current source. The current source was connected between the metal counterelectrode and one of the metallic contacts on the bar. The dc bias and ac voltage across the junction were picked up between the counterelectrode and the other metallic contact. This essentially “three poles” method eliminates possible errors introduced by higher resistivity of the metallic contacts. The ac voltage was detected by a lock-in amplifier and plotted as a function of bias.

As discussed in detail by Conley and Mahan,<sup>7</sup> when certain conditions are fulfilled, the resistance  $dV/dI$  peaks at a forward bias equal to  $\mu_F$  the Fermi energy. It was shown in a previous publication<sup>3</sup> that in the case of semiconducting  $\text{SrTiO}_3$ , the peak of resistivity should really occur at  $\mu_F$ . The measured carrier-concentration dependence<sup>3</sup> of the position of the peak supports this conclusion.

To provide further evidence, we have measured  $dV/dI$  versus the bias  $V$  on  $\text{In-KTaO}_3$ : Ca junctions and have compared the results with measurements on  $\text{In-SrTiO}_3$ : Nb junctions. In both materials the carrier concentrations were practically the same. The resulting curves are shown in Fig. 1. For each curve the maximum occurs at the applied bias which corresponds to the Fermi energy of the semiconductor. For  $\text{SrTiO}_3$  (carrier concentration  $n = 7 \times 10^{18}/\text{cm}^3$ ), the maximum occurs at the bias  $10 \pm 2$  meV and for  $\text{KTaO}_3$  ( $n = 8 \times 10^{18}/\text{cm}^3$ ) at the bias  $21 \pm 3$  meV. Inserting these values in the usual relationship

$$\mu_F = (\hbar^2/2m_d)(3\pi^2n)^{2/3}, \quad (1)$$

we determined  $m_d$  quantitatively,

$$\begin{aligned} m_d(\text{SrTiO}_3) &= (1.3 \pm 0.2)m_0, \\ m_d(\text{KTaO}_3) &= (0.69 \pm 0.1)m_0, \end{aligned} \quad (2)$$

where  $m_0$  is the free-electron mass.

The value of  $m_d$  in  $\text{KTaO}_3$  can be compared to the published value  $m_d \approx 0.8 m_0$  inferred from cyclotron resonance,<sup>1</sup> thermopower measurement,<sup>5</sup> and Faraday rotation.<sup>8</sup> The good agreement between the two values provides experimental evidence that

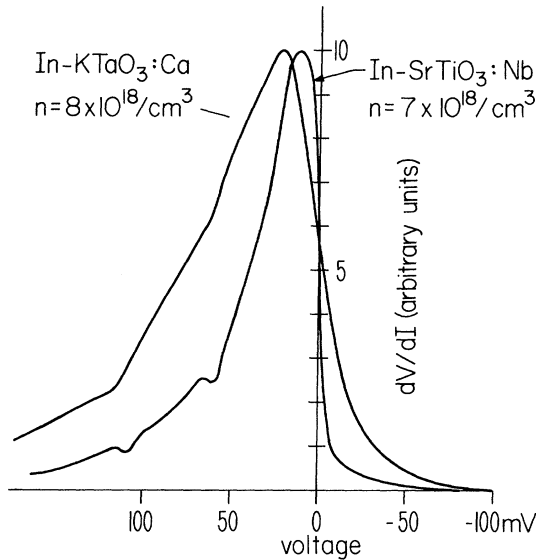


FIG. 1. Dynamic resistivity plotted versus applied bias for In-SrTiO<sub>3</sub>:Nb and In-KTaO<sub>3</sub>:Ca junctions. The positions of the maximum of the curves correspond to the Fermi energies of the semiconductors. The structure at about 60 and 100 mV is due to interaction of tunneling electrons with LO phonons of SrTiO<sub>3</sub> and KTaO<sub>3</sub> (Ref. 3).

the tunneling technique is a reliable method for the direct observation and quantitative measurement of degeneracy in perovskite semiconductors.

Another advantage offered by the tunneling technique is the possibility of experiments at higher temperature. Provided that tunneling is the prevailing transport mechanism through the barrier at all temperatures, the technique can be used to measure directly the temperature dependence of effective mass. At this point, it should be mentioned that tunneling through Schottky barriers, as used, for example, in our experiments, is not the best tunneling method for the measurement of Fermi energy at higher temperatures. The potential in the depletion region has a parabolic dependence so that the transition probability through the barrier is very sensitive to the energy of electrons. Consequently, the temperature smearing of the Fermi energy of the metal may effectively move the position of the resistivity peak and mask possible changes of the semiconductor Fermi energy.

The tunneling characteristics of In-SrTiO<sub>3</sub>:Nb junctions at different temperatures are shown in Fig. 2. The samples with high carrier concentration  $n = 5 \times 10^{19}/\text{cm}^3$  have been used. Despite the striking changes of the characteristics with temperature, the position of the peak at the Fermi energy (+45 mV), and consequently also the effective mass, are temperature independent at least up to 77 °K.

Small shifts of the resistivity peak toward smaller biases, observed at temperatures above 100 °K (not shown in Fig. 2), could be attributed to the parabolic dependence of the barrier potential as mentioned above and was not studied in detail.

The origin of the small but distinct peak of resistivity in Fig. 2 at reverse biases (minus voltage), and its strong temperature dependence, is presently not understood. The characteristic is well reproducible and does not depend upon the technology of junction fabrication. Unfortunately, we were not able to carry out similar experiments at high reverse biases on lightly doped samples. The resistivity of the junctions with lightly doped SrTiO<sub>3</sub> goes to zero at reverse biases very fast and the sensitivity is too small.

In conclusion, we may say that our experiments indicate that the peak of resistivity at forward biases in junctions with doped SrTiO<sub>3</sub> and KTaO<sub>3</sub> occurs at biases equal to the Fermi energy of the semiconductor. The peak reflects the critical point in the density of states at the bottom of the semiconductor conduction band. However, the structure at reverse biases remains unexplained. Strong temperature dependence excludes the possibility that the structure is due to single-phonon or plasmon interactions in the bulk or in the depletion area.

### III. CONDUCTION-BAND STRUCTURE OF SrTiO<sub>3</sub>

To obtain information about the mass tensors in

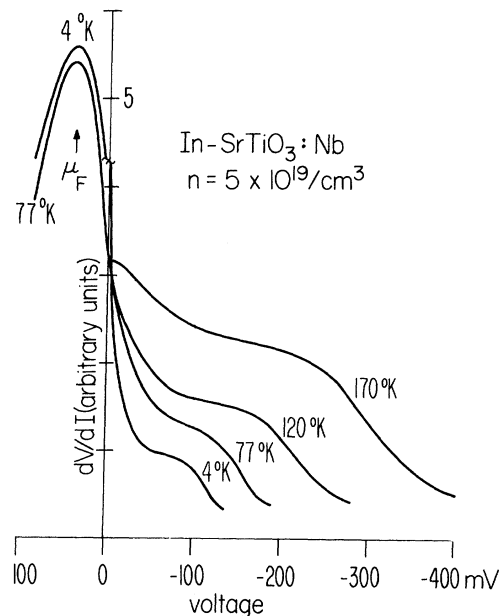


FIG. 2. Dynamic resistivity of In-SrTiO<sub>3</sub>:Nb at different temperatures. For positive bias at 4 °K, the gain of the chart recorder was reduced by a factor of 2.

SrTiO<sub>3</sub> and KTaO<sub>3</sub>, the values of  $m_d$  in (2) should be combined with magnetoresistance data.<sup>2,9</sup> The interpretation of the magnetoresistance measurements is consistent in both materials with an electron-energy surface consisting of three spheroids along the  $\langle 100 \rangle$  crystal axes, with a mass anisotropy ratio  $K (= m_l/m_t)$  of around 4.

Assuming the relationship

$$m_d = (3)^{2/3} (m_t^2 m_l)^{1/3}, \quad (3)$$

where  $m_l$  and  $m_t$  are longitudinal and transversal masses, respectively, we obtain

$$\begin{aligned} \text{SrTiO}_3: m_l &= 1.6m_0 \quad (\Delta_l = 0.54 \text{ eV}), \\ m_t &= 0.4m_0 \quad (\Delta_t = 2.2 \text{ eV}); \end{aligned} \quad (4)$$

$$\begin{aligned} \text{KTaO}_3: m_l &= 0.84m_0 \quad (\Delta_l = 1 \text{ eV}), \\ m_t &= 0.21m_0 \quad (\Delta_t = 4.3 \text{ eV}). \end{aligned} \quad (5)$$

The values in brackets are the corresponding bandwidths in the tight-binding approximation.

The purpose of the discussion below is to discuss a model of the SrTiO<sub>3</sub> conduction band and fit it to the presented experimental data.

The basic understanding of the band structure of SrTiO<sub>3</sub> is due to Kahn and Leyendecker,<sup>4</sup> and the reader is referred to their article for references and nomenclature. They have applied the LCAO or tight-binding method, employing, whenever possible, empirical data to fix the parameters of the SrTiO<sub>3</sub> problem. The main conclusion of their calculation is that the lowest conduction band is formed by threefold degenerate  $t_{2g}$ - $3d$  wave functions, with six ellipsoids lying along  $\langle 100 \rangle$  directions of  $k$  space with minima at the edges of Brillouin zone. The edge of the broader  $e_g$  band lies about 0.6 eV above the bottom edge of the  $t_{2g}$  band. The lowest conduction band  $\Delta'_2$  is flat along the cubic axes, i. e., the longitudinal mass is infinite. The transversal mass is determined by the  $M_5$ - $X_3$  separation and is approximately equal to the free-electron mass  $m_0$ . Inclusion of Ti-Ti overlap would cause the lowest conduction band  $\Delta'_2$  to curve downward along the cubic axes, depressing the band at the edge of the Brillouin zone by about 20–50 mV, corresponding to the value of  $m_l \cong (50 - 20)m_0$ .

According to our measurement, both ( $m_l$  and  $m_t$ ) masses are substantially smaller than those predicted from the Kahn-Leyendecker model and we have reconsidered the basic assumption that the relatively narrow  $t_{2g}$  band is lowest. This assumption in the paper of Kahn and Leyendecker was based on the observation that the  $\Gamma_{12}(e_g)$ - $\Gamma_{25}(t_{2g})$  splitting at  $\vec{k} = 0$  is essentially the crystal field splitting of  $e_g$ - $t_{2g}$  orbitals, similar in nature to the  $10Dq$  splitting appropriate to localized  $d$  elec-

trons. Kahn and Leyendecker calculated the  $\Gamma_{12}$ - $\Gamma_{25}$  splitting in a point-charge approximation using Watson's Ti<sup>3+</sup> Hartree-Fock wave functions and found  $\Gamma_{12}$ - $\Gamma_{25} = +0.6$  eV (the  $t_{2g}$  band being lowest for a positive sign of the splitting).

We have recalculated the  $\Gamma_{12}$ - $\Gamma_{25}$  splitting using a microscopic analysis of individual contributions to the  $e_g$ - $t_{2g}$  ( $10Dq$ ) splitting of localized  $d$  orbitals.<sup>10</sup> It is well established that this ( $10Dq$ ) splitting is caused by the so-called diagonal terms, nonorthogonality terms, and covalency.<sup>10</sup> The numerical magnitude of the last two very important terms is rather sensitive to the tails of the wave functions, and attempts to calculate  $10Dq$  have therefore enjoyed only limited success. Fortunately, the delocalized  $3d$ -band wave functions at  $\vec{k} = 0$ ,  $\Gamma_{12}(e_g)$  and  $\Gamma_{25}(t_{2g})$  are orthogonal to all  $2p$  oxygen wave functions ( $\Gamma_{15}$ ,  $\Gamma_{25}$ ,  $\Gamma_{15}$ ), which results in a vanishing of the large  $3d$ - $2p$  covalency and nonorthogonality contributions to the  $\Gamma_{12}$ - $\Gamma_{25}$  splitting. What remains at  $\vec{k} = 0$  are only the diagonal and the  $3d$ - $2s$  covalency and nonorthogonality terms.

The diagonal terms, essentially, the point-charge contribution, the exchange contribution, and Kleiner's correction, can be calculated with reasonable precision using Hartree-Fock wave functions of O<sup>2-</sup> and Ti<sup>3+</sup>. The point-charge contribution to  $\Gamma_{12}$ - $\Gamma_{25}$  has already been calculated by Kahn and Leyendecker,<sup>4</sup> and found to be +0.62 eV. We have estimated numerically the Kleiner's correction and exchange contribution to be -0.4 and -1 eV, respectively. The resulting diagonal contribution is -0.8 eV. The magnitude of this estimate is probably not very sensitive to the specific wave functions we have used, because if more expanded wave functions were used the point-charge contribution would increase but so would the negative contributions from Kleiner's correction and the exchange interaction. At this point it should be mentioned that even for the (NiF<sub>6</sub>)<sup>-4</sup> complex where the  $3d$  wave functions of Ni<sup>2+</sup> and the  $2p$  wave functions of F<sup>-</sup> are relatively very contracted and one expects the positive point charge to be predominant, the actual sum of diagonal contributions is negative and equal to -0.44 eV.

The  $3d$ - $2s$  nonorthogonality contribution to the  $\Gamma_{12}$ - $\Gamma_{25}$  splitting can be evaluated easily, using the method introduced by Sugano and Shulman.<sup>10</sup> The actual value turns out to be small and *negative* ( $\cong -0.2$  eV) in contrast to the large positive contribution (+0.5 eV) in (NiF<sub>6</sub>)<sup>-4</sup> complex.<sup>10</sup> The numerical calculation of the definitely positive  $3d$ - $2s$  covalency contribution is, however, with our present knowledge of O<sup>2-</sup> wave functions in the solid state, practically impossible, and was not attempted. In view of the fact that  $2s$  levels are centered  $\sim 15$  eV below the  $2p$  oxygen levels, the covalency contribution is believed to be very small in SrTiO<sub>3</sub>. The value

of +0.5 eV is set as an upper limit for the sum of both  $3d$ - $2s$  overlap and covalency contributions.

The resulting splitting of  $\Gamma_{12}$ - $\Gamma_{25'}$  is the sum of diagonal and  $3d$ - $2s$  covalency contributions with an upper-limit value of

$$\Gamma_{12} - \Gamma_{25'} = -0.3 \text{ eV},$$

the  $e_g$  band being now lowest at  $\vec{k}=0$ .

In this scheme, the transversal mass  $m_t$  is determined by the width of the  $Z_1$ - $3d$  band ( $M_1$ - $X_2$  separation.) Our experimental value 2 eV of the  $M_1$ - $X_2$  separation is quite reasonable.<sup>4</sup> The small value of the longitudinal mass  $m_l = 2m_0$  may also now be better understood. The  $\Delta_2$ - $3d$  wave functions which determine the value of  $m_l$  in this scheme can be mixed by symmetry with oxygen  $s$  functions and, consequently, are spread more in space than  $\Delta_2'$  (pure  $3d$ ) functions. As the result, the  $\Delta_2$  band is expected to be curved more than  $\Delta_2'$ , leading to small value of  $m_l$ .

The proposed conduction-band structure of  $\text{SrTiO}_3$  for the wave vectors  $\vec{k}$  along the  $[100]$  cubic axis is shown in Fig. 3. For the  $\Gamma_{12}$ - $X_2$  separation our experimental value 0.5 eV has been used and the  $X_1$ - $\Gamma_{12}$  has been determined from the experimental value  $M_1 - X_2 = 2$  eV, using the relation  $X_1 - \Gamma_{12} = \frac{16}{9} \times (M_1 - X_2)$ . The relation is a consequence of the cubic symmetry of the problem. The curvatures of  $t_{2g}$  bands ( $\Delta_2'$  and  $\Delta_5$ ) was reproduced from the Kahn-Leyendecker calculation.

To conclude this section, we should point out that we have discussed the conduction-band structure of  $\text{SrTiO}_3$  strictly in the framework of the LCAO approximation. Nevertheless, we believe that the suggested "inversion" of  $3d$  states at  $\vec{k}=0$  from the dilute compound order is the crystal field splitting problem and is not very sensitive to the method of band calculation. The calculated numerical value of the splitting  $\Gamma_{12} - \Gamma_{25'} = -0.3$  eV should be taken as tentative in view of the approximations used. The actual value depends critically upon the balance between the negative crystal field contribution discussed above and the positive  $3d$ - $2s$  covalency contribution. The outlined calculation merely shows that the positive  $3d$ - $2s$  covalency and point-charge contributions to  $\Gamma_{12} - \Gamma_{25'}$  splitting are compensated or even overcompensated by negative diagonal terms (exchange and Kleiner's corrections) and overestimates the actual value of the splitting. The isolated ion  $2p$  covalent and overlap contributions which normally overcome this negative value for dilute paramagnetic salts are absent by symmetry at  $\vec{k}=0$  in pure translationally invariant transition-metal compounds with perovskite structure.

#### IV. DISCUSSION

Using the tunneling method we have measured the

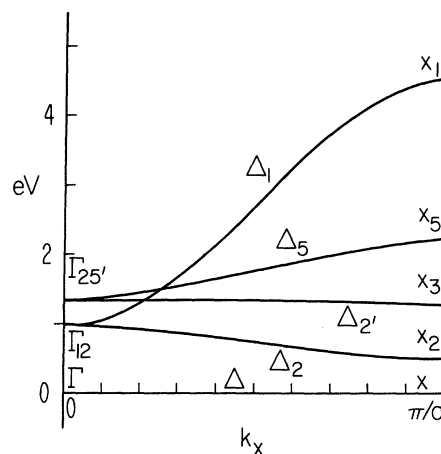


FIG. 3. Plot of energy of conduction electrons of  $\text{SrTiO}_3$  versus wave vector for  $\vec{k}$  along the  $[100]$  direction. The separations  $\Gamma_{12} - X_2$  and  $X_1 - \Gamma_{12}$  are deduced from the experiments, the  $X_5 - \Gamma_{25'}$  and  $\Gamma_{25'} - X_3$  are taken from Ref. 4.

density-of-states effective mass of two perovskite semiconductors  $\text{SrTiO}_3$  and  $\text{KTaO}_3$ . The data for  $\text{KTaO}_3$  agree reasonably well with the cyclotron-resonance and Faraday rotation measurements.<sup>1,8</sup> On the other hand, the density-of-states effective mass of  $\text{SrTiO}_3$  reported in this paper ( $1.3m_0$ ) differs substantially from the density-of-states effective mass ( $4m_0$ ) previously obtained from spin-susceptibility measurements.<sup>11</sup> In view of the fact that the Fermi energies for the doping level of  $\text{SrTiO}_3$  in our experiments are far below the LO-phonon energies, the polaron corrections cannot explain the large discrepancy between these two measurements, nor can the nonparabolicity of the bands be responsible since no deviation from parabolic law has been found by spin-susceptibility and tunneling measurements in the relevant concentration range. We suggest that the discrepancy is caused by the presence in the measured free-carrier-electron susceptibility of Van Vleck paramagnetism, which leads to an apparent higher density of states at the Fermi level.

The masses of free carriers in  $\text{SrTiO}_3$  and  $\text{KTaO}_3$  reported in this article are in the same ratio (2) as the ratio of inverse values of  $10Dq$  of  $\text{Ti}^{3+}$  ( $10Dq \approx 20\,000 \text{ cm}^{-1}$ ) and  $\text{Ta}^{4+}$  ( $10Dq \approx 40\,000 \text{ cm}^{-1}$ ). This is consistent with the similar microscopic origin of  $10Dq$  and the conduction bandwidths.

The observation of small effective masses in both material suggests the possibility that instead of the  $t_{2g}$ , the broader  $e_g$  band is the lowest conduction band. From experiment alone, one cannot decide unambiguously which band is lowest. The final decision depends presently upon the quantitative calculation of the  $\Gamma_{12} - \Gamma_{25'}$  separation. The calculation in the theoretical part of this paper is a relatively

exact numerical evaluation of all the microscopic contributions to  $\Gamma_{12} - \Gamma_{25'}$  splitting (except  $2s-3d$  covalency). Because of spatial symmetry, the  $3d-2p$  transfer plays no role. The resulting calculated value of the  $\Gamma_{12} - \Gamma_{25'}$  splitting is negative ( $e_g$  lower) and the crystal field contribution is rather insensitive to the wave functions.

It is interesting to compare our results with the recent augmented plane-wave (APW) calculation of the band structure of  $\text{ReO}_3$  by Mattheiss.<sup>12</sup> The crystallographic and electronic structures of  $\text{ReO}_3$  are very similar to that of  $\text{SrTiO}_3$  and  $\text{KTaO}_3$ , and consequently, the basic qualitative results of band calculation are expected to be the same for all three materials. Mattheiss calculates a value<sup>12</sup> of the  $\Gamma_{12} - \Gamma_{25'}$  splitting in  $\text{ReO}_3$  which is positive and equal to 3.9 eV, 2.6 eV being due to the  $5d-2s$  covalency and 1.3 eV due to crystal potential. The latter contribution, which was calculated using the corrections to the "muffin-tin" potential is equivalent to the diagonal term discussed in this paper and which for  $\text{SrTiO}_3$  turns out to be negative. The discrepancy is certainly due to the use of different

potentials. Because the corrections to the muffin-tin potential (atomic Coulomb interaction and Slater average exchange potential) do not mirror sufficiently accurately the microscopic character of the crystal field potential, the APW calculation of this particular problem of crystal field contribution to the  $\Gamma_{12} - \Gamma_{25'}$  splitting should be compared with the quantitative theory outlined above. The same is true for the APW calculation of  $\Gamma_{12} - \Gamma_{25'}$  splitting in  $\text{SrTiO}_3$  mentioned briefly in Ref. 12. The results of such an analysis may be even more important in transition-metal oxide with rocksalt structure (TiO and VO), because in these materials, the  $d$  functions at  $k=0$  are orthogonal to both  $2p$  and  $2s$  oxygen wave functions and the positive contribution of  $2s-3d$  covalency is missing.

#### ACKNOWLEDGMENT

The author is grateful to Professor R. Orbach for many suggestions and interest in this work and Professor T. Holstein, Professor P. Pincus, Professor E. Simanek, Professor Nai Li Huang, and Professor N. Rivier for helpful discussions.

<sup>†</sup>Work supported in part by the National Science Foundation.

<sup>\*</sup>On leave from the Institute of Radio Engineering and Electronics, Czechoslovak Academy of Science, Prague, Czechoslovakia.

<sup>1</sup>L. S. Senhouse, G. E. Smith, and M. V. De Paolis, *Phys. Rev. Letters* **15**, 776 (1965).

<sup>2</sup>W. R. Hosler and H. P. R. Frederikse, *Solid State Commun.* **7**, 1443 (1969).

<sup>3</sup>Z. Sroubek, *Solid State Commun.* **7**, 1561 (1969).

<sup>4</sup>A. H. Kahn and A. J. Leyendecker, *Phys. Rev.* **135**, A1321 (1964).

<sup>5</sup>S. H. Wemple, *Phys. Rev.* **137**, A1575 (1965).

<sup>6</sup>D. M. Hannon, *Phys. Rev.* **164**, 366 (1967).

<sup>7</sup>J. W. Conley and G. D. Mahan, *Phys. Rev.* **161**, 681 (1967).

<sup>8</sup>W. S. Baer, *Phys. Rev. Letters* **16**, 729 (1966).

<sup>9</sup>H. P. R. Frederikse, W. R. Hosler, and W. R. Thurber, *Phys. Rev.* **143**, 648 (1966).

<sup>10</sup>S. Sugano and R. G. Shulman, *Phys. Rev.* **130**, 517 (1963).

<sup>11</sup>H. P. R. Frederikse and G. A. Candela, *Phys. Rev.* **147**, 583 (1966).

<sup>12</sup>L. F. Mattheiss, *Phys. Rev.* **181**, 987 (1969).

## Transverse Magnetoconductivity in $n$ -Type Germanium<sup>†\*</sup>

P. K. Govind<sup>‡</sup> and S. C. Miller

*Department Of Physics and Astrophysics, University of Colorado, Boulder, Colorado 80302*

(Received 22 April 1970)

A quantum-mechanical calculation of transverse magnetoresistance is made for an electron gas with anisotropic effective mass. For acoustic-phonon scattering, numerical calculations are made with parameters appropriate to the conduction band of  $n$ -Ge in the temperature range 30–77°K with magnetic fields up to 200 kG. For high magnetic fields there is a quantitative disagreement between theory and experiment which is not understood at present.

### I. INTRODUCTION

There has been a relatively small amount of experimental work on high magnetic field transverse magnetoresistance in semiconductors. This

is largely due to the belief of many investigators that effects of inhomogeneities are greater than those of fundamental scattering mechanisms. However, the experiments of Gallagher and Love<sup>1</sup> suggested that inhomogeneity effects might not be